Published in: Applied Materials & Interfaces (2021), vol. 13, pp. 54396–54408
DOI: 10.1021/acsami.1c16917
Status : Postprint (Author's version)

INTRODUCING POLYHYDROXYURETHANE HYDROGELS AND COATINGS FOR FORMALDEHYDE CAPTURE

Maxime Bourguignon

Center for Education and Research on Macromolecules (CERM), CESAM Research Unit, University of Liege, 4000 Liege, Belgium.

Bruno Grignard

Center for Education and Research on Macromolecules (CERM), CESAM Research Unit, University of Liege, 4000 Liege, Belgium.

Christophe Detrembleur*

Center for Education and Research on Macromolecules (CERM), CESAM Research Unit, University of Liege, 4000 Liege, Belgium.

ABSTRACT: Formaldehyde (FA) is a harmful chemical product largely used for producing resins found in our living spaces. Residual FA that leaches out the resin contributes to our indoor air pollution and causes some important health issues. Systems able to capture this volatile organic compound are highly desirable; however, traditional adsorbents are most often restricted to air filtration systems. Herein, we report novel waterborne coatings that are acting as a FA sponge for indoor air decontamination. These coatings, of the poly(hydroxyurethane) (PHU) type, rich in primary amine groups, are prepared by the polyaddition of a hydrosoluble dicyclic carbonate to a polyamine in water at room temperature under catalyst-free conditions. We highlight the importance of the choice of the polyamine on the curing rate of the formulation and on the FA capture ability of PHU. The excellent FA capturing ability of the best candidate is rationalized by investigating the action mode of the polyamine used to construct PHUs. With poly(vinyl amine), FA is covalently and permanently bound to PHU, with no release over time. The performance of the coating in FA abatement is impressive, with more than 90% of captured FA after one day of contact. The facility to prepare these transparent and colorless coatings from waterborne formulations gives access to new efficient indoor air depolluting solutions, potentially applicable to various surfaces of our living spaces (wall, ceiling, etc.).

Published in: Applied Materials & Interfaces (2021), vol. 13, pp. 54396–54408
DOI: 10.1021/acsami.1c16917
Status : Postprint (Author's version)

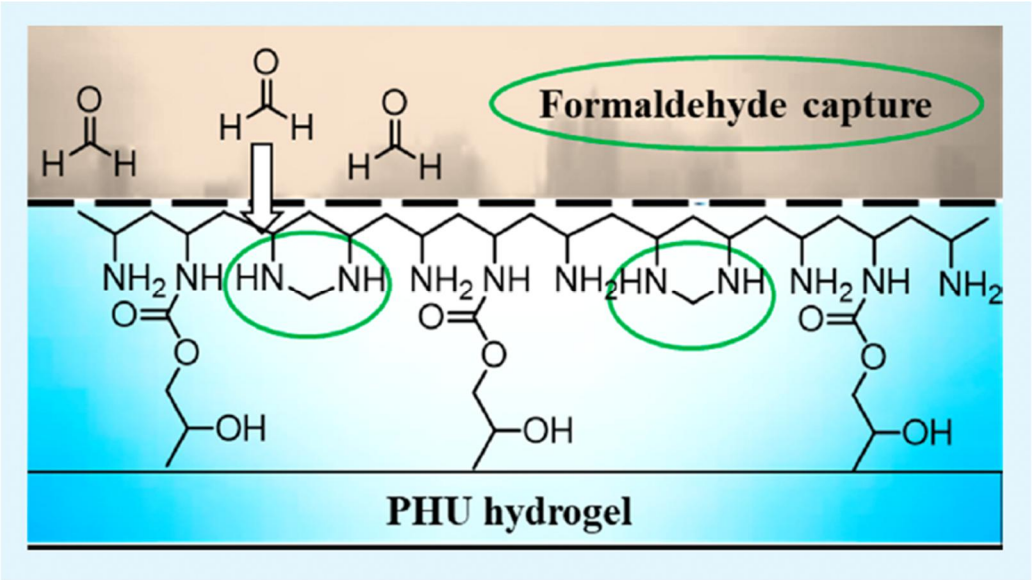

KEYWORDS: **nonisocyanate polyurethane, polyvinylamine, cyclic carbonate, solvent-free formulation, indoor air purification.**

INTRODUCTION

Formaldehyde (FA), a colorless gas under ambient condition, is largely used in chemical industries and, in particular, in the manufacture of synthetic resins (urea formaldehyde and melamine urea formaldehyde, melamine formaldehyde) found in many daily-life applications (e.g., furniture, carpet, flooring, coatings). Residual FA is however continuously released from these products and accumulates in closed areas such as schools, houses, workspace, etc. As FA is highly hydrophilic, its absorption by human respiratory or gastrointestinal tracks is facile. Its high reactivity toward a large variety of chemical functions (e.g., amines) promotes its binding to biological tissues causing serious pathogenicity like headaches, asthma, cancer.[1−3] Therefore, the World Health Organization recommends to limit the formaldehyde concentration in residential indoor air to 0.8 ppm[4] and to below 0.2 ppm for workers manipulating this gas during complete work life, to 0.75 ppm for an 8 h/day or 40 h/week, and to 2 ppm for 15 min exposure.[5]

Several methods to decrease FA concentration in indoor air emerged recently to tackle these objectives. The first solution consists of reducing the FA emission from high formaldehyde containing resins by the addition in the resin formulation of FA scavengers like amines,[6,7] tannin,[8−10] urea,[11,12] Al_2O_3 nanoparticles, [13] or sodium metabisulfite.[12] However, such changes may impart a strong modification of the resin properties or affect the application process.[6,8] Other solutions consist of eliminating FA after its emission. In this case, the (photo)-catalytic oxidation, bioremediation, or adsorption in various substrates are the most widely investigated techniques.[14] In the photocatalytic approach, the most preferred TiO_2 promotes the transformation of FA into CO_2 and water under UV light irradiation.[15−20] Advantageously, this technique is compatible with humidity since the presence of water tends to increase the degradation capacity of the catalyst.[21] The catalytic oxidation uses noble-metal or oxide catalysts embedded within (in)-organic or metallic matrices,[15,22] and also turns FA into CO_2 and water.

Published in: Applied Materials & Interfaces (2021), vol. 13, pp. 54396–54408
DOI: 10.1021/acsami.1c16917
Status : Postprint (Author's version)

Although promising, room-temperature degradation of FA is only possible with some expensive noble-metal catalysts[22–26] and their efficiency was not proven at a low FA concentration (<ppm).[15,22] (Photo)catalytic oxidation methods are however nonselective to FA and degrade any organic compounds with the formation of radicals able to react with other substances with the risk of formation of harmful byproducts.[18,27] On the other hand, the enzymatic bioremediation is highly selective to FA and can convert this waste into nontoxic products under ambient conditions. In this field, compost extracts,[28] i.e., FA-degrading microorganisms like fungi[29,30] or bacteria,[31] or purified specific enzymes were employed for FA abatement.[32] However, maintaining the stability and activity of the biocatalyst is challenging under gaseous conditions,[28,32] which currently limits their use to FA waste water remediation. Besides, the FA adsorption in (in)organic matrices is often exploited as a low-cost and simple alternative technique for VOC abatement. Unlike (photo)catalytic oxidation and bioremediation, the gas is not decomposed but (permanently) sequestered within the material. Activated carbons, potentially doped by metals (aluminum, silver, or copper), permitted the capture of FA.[33–38] Nevertheless, with these systems, the presence of humidity was detrimental to the FA adsorption,[39–41] the condensed water limiting the FA diffusion into the absorbent. Other inorganic porous substrates such as silicas, phosphates, or aluminosilicates were also used.[42] The modification of the outer surface of the absorbents by amino groups increased their FA capture capacity.[34,36,41,43–45] Although not fully clear yet, the formation of a Schiff base adduct by reaction with FA was suggested for this improved FA abatement.[36,46] Finally, carboxylic acid-functionalized terpyridine/KOH-based hydrogels were also reported for their ability to capture FA and to degrade it into nontoxic salts such as HCOOK and CH_3OK.[47] Surprisingly, only a few studies were dedicated to the use of polymer matrices for FA capture, while multiple examples are found for other VOCs, e.g., hexane,[48] chlorinated VOCs,[49] methyl ethyl ketone,[50] benzene,[50,51] or alcohols.[52] Rare examples of FA capture were reported for polymer coatings containing polyethyleneimine (PEI),[31] chitosan,[53–56] secondary amine,[57] or other pendant primary amines.[58]

Recently, we reported the polyaddition of polyamines to polycyclic carbonates for producing nonisocyanate polyurethanes hydrogels at room temperature without using any organic solvent nor toxic isocyanates.[59,60] These hydrogels, of the poly(hydroxyurethane) (PHU) type, were directly prepared in water under ambient conditions with short gel times, and their properties were easily tuned on-demand by adapting the nature of the polyamines and polycyclic carbonates, their composition, and also by introducing inorganic (e.g., clay) or natural fillers (e.g., gelatin). We hypothesize that these PHU hydrogels present a serious potential for developing depolluting coatings for FA capture, especially for PHU hydrogels bearing a high content of pendent amines.

In this work, we engineered novel amino-functionalized hydrophilic PHU coatings/hydrogels for FA capture. To design the best-performing depolluting material, we first establish the relationship between the PHU microstructure and its FA capture potential prior to extending the utilization of these new materials to capture formaldehyde in aqueous or gaseous conditions.

Published in: Applied Materials & Interfaces (2021), vol. 13, pp. 54396–54408
DOI: 10.1021/acsami.1c16917
Status : Postprint (Author's version)

EXPERIMENTAL SECTION

Synthesis of Poly(hydroxyurethane) (PHU) Hydrogels and Coatings. In a representative experiment, polyvinylamine (PVam, 17 mg, NH_2 = 0.4 mmol) was solubilized in 0.8 mL of water after vigorous stirring and the pH was adjusted to 10 using HCl 35%. The PVam solution was then added to poly(ethylene glycol) dicyclic carbonate (PEG-di5CC, 33 mg, 5CC = 0.1 mmol) diluted in 200 μL and then stirred for 30 s. The solution was then placed into a plastic mold or onto a stainless steel plate with a bar coater (200 μm thickness, using Garco Microm II bar coater system). The mixture is left to cross-link at room temperature.

Model Reaction between PVam and Ethylene Carbonate. In a representative experiment, poly(vinyl amine) (PVam, 17 mg, NH_2 = 0.4 mmol) was solubilized in 0.8 mL of deuterated water (D_2O) after vigorous stirring, and the pH was adjusted to a desired value (8.5 or 10) using DCl 35%. The PVam solution was then added to ethylene carbonate (EC, 8.8 mg, 5CC = 0.1 mmol) diluted in 200 μL of water and then stirred for 30 s. Crude product was purified by precipitation in 10 mL of acetone. The precipitate was recovered and dried under vacuum for 24 h at 40 °C.

Preparation of NASH Test Reactant. Ammonium acetate (750 mg, 9.7 mmol), acetyl acetone (10 μL, 0.97 mmol), and glacial acetic acid (15 μL, 0.16 mmol) were mixed in 5 mL of water just before testing.

Formaldehyde Capture Assays by Amines. The amine solution in water (0.56 M) was adjusted at desired pH values (i.e., pH = 10.5, 8.5, 7.2, and 3.5) by the addition of concentrated HCl (12M). Formaldehyde was quantified by the colorimetric NASH test following the standard procedure. Formaldehyde (0.1 mL at 10 mM in water) was added to the solution containing the amine (900 μL) to reach a final concentration in FA of 1 mM. The solution was left to react at room temperature in a closed glass vial to avoid evaporation. The sample (160 μL) was picked out and added to 160 μL of the solution of the freshly prepared NASH reagent. The mix was reacted 10 min at 60 °C before analyzing by UV spectroscopy at 412 nm. All experiments were carried out in triplicate. Results are presented in Figure 1.

Published in: Applied Materials & Interfaces (2021), vol. 13, pp. 54396–54408
DOI: 10.1021/acsami.1c16917
Status : Postprint (Author's version)

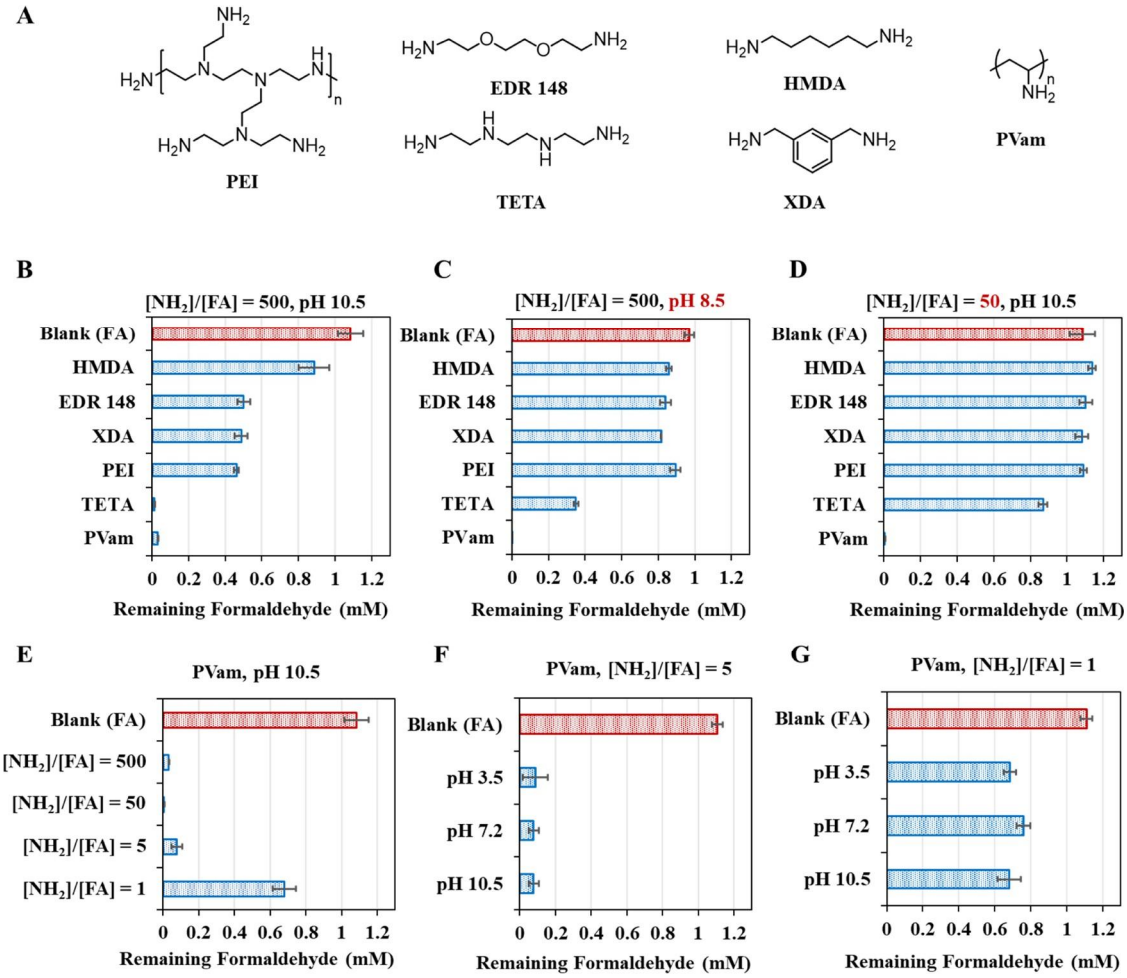

Figure 1. Formaldehyde capture experiments by various amines and under various conditions. (A) Structures of the different tested amines. FA capture efficiency by different amines (B) at pH = 10.5 for $[NH_2]/[FA]$ = 500, (C) at pH = 8.5 for $[NH_2]/[FA]$ = 500, and (D) at pH = 10.5 for $[NH_2]/[FA]$ = 50. (E) Influence of $[NH_2]/[FA]$ molar ratio on FA capture by PVam at pH = 10.5. (F) Influence of pH on FA capture by PVam for $[NH_2]/[FA]$ = 5. (G) Influence of pH on FA capture by PVam for $[NH_2]/[FA]$ = 1. Conditions: 1 h of incubation in water at rt, [FA] = 1 mM.

Capture of Formaldehyde by PHU Hydrogels. PHU hydrogels were prepared by mixing PVam solution (4.25 mg, NH_2 = 0.1 mmol, in 0.2 mL of water, pH 10) with PEG-di5CC solution (8.25 mg, 5CC = 0.025 mmol in 0.05 mL of water) in a 24-well plate for 24 h according to the procedure described above. Then, 1 mL of a solution containing FA (1 mM) was added on the PHU coating. The mixture is left to react at room temperature in a closed vial to avoid evaporation. The supernatant (160 µL) was picked out and added to 160 µL of the NASH reagent. The solution was reacted 10 min at 60 °C before analyzing by UV spectroscopy at 412 nm. The concentration in FA was determined using a formaldehyde calibration curve (ranging from 0.05 to 1 mM in FA by dilution of FA in water, Figure S25). All of the experiments were carried out in triplicate. Results are summarized in Figure 6B.

Published in: Applied Materials & Interfaces (2021), vol. 13, pp. 54396–54408
DOI: 10.1021/acsami.1c16917
Status : Postprint (Author's version)

Assessment of FA Released by PHU Hydrogels. PHU hydrogels were prepared by mixing PVam solution with PEGdi5CC solution in a 24-well plate for 24 h according to the procedure described above. Then, 1 mL of solution containing FA (1 mM) was added on the PHU hydrogel and was left to react for 1 h at 25 °C in a closed vial. The amount of captured formaldehyde was calculated using NASH test as described above. After removing the supernatant, 1 mL of water was added on the hydrogel to extract unbonded FA. The released FA was measured after 24 and 48 h by the NASH test. For that purpose, 160 μL of the supernatant was picked out and added to 160 μL of the NASH reagent. The solution was reacted 10 min at 60 °C before analyzing by UV spectroscopy at 412 nm. The concentration of FA was determined according to the calibration curve presented in Figure S25. All experiments were carried out in triplicate. Results are summarized in Figure 6C.

Gaseous Formaldehyde Capture and Release Assay. PVam (25 mg, NH_2 0.6 mmol) was solubilized in 1 mL of water, and pH was adjusted to 10 with concentrated HCl. The PVam solution was added to a PEG-di5CC solution (49 mg, 5CC = 0.15 mmol in 350 μL of water) and was mixed before coating on a stainless steel plate (15 cm × 5 cm, 10 g of PHU/m^2) with a bar coater (200 μm thickness, using Garco Microm II bar coater system). The coating was then dried at room temperature for 24 h. Gaseous FA assay was carried out according to a standard protocol as described below.[2,58] An emission vial with FA (5 mL, 10 mM in water), a reception vial with water (5 mL), and a stainless steel surface coated by PHU was placed in a plastic container that was hermetically closed. The system was left to equilibrate for different times (24 h, 3 days, or 7 days). Then, 160 μL of the reception vial was picked out and mixed with 160 μL of the Nash reagent. The solution was reacted 10 min at 60 °C before analyzing at 412 nm by UV spectroscopy. The concentration of FA was determined using a calibration curve presented in Figure S25. The emission and reception vial were replaced between each measurement. All experiments were carried out in triplicate. Results are summarized in Figure 7.

For FA release assays, the emission vial containing FA was removed after 16 days of capture, and PHU coatings used for FA capture were left to equilibrate for 1 and 4 days at room temperature in the presence of a reception vial containing 5 mL of water in the same closed vial. The concentration of FA in the reception vial was measured according to the same procedure. Results are presented in Figure S23B. The procedure for FA release at 40 °C is described in Section 12.2 in the Supporting Information.

Thermal and Mechanical Analyses of PHU Films before and after FA Capture. PHU films were prepared by casting 5 mL of a solution of PVam (17 mg/mL) and PEG-di5CC (33 mg/mL) at pH 10 into a plastic mold (surface = 23 cm^2). The films were left to dry under ambient condition for 24 h. Formaldehyde (20 mL, 1 mM or 10 mM) was added on PHU films for 1 h to promote FA capture by the films. The supernatant was discarded, and the coating was left to dry for 48 h. The films were peeled off and then analyzed by thermogravimetric analysis (TGA) and differential scanning calorimetry (DSC). TGA was performed on a TGA2 instrument from Mettler Toledo. Around 10 mg of the sample was heated at 10 °C/min until 600 °C under a nitrogen atmosphere (50 mL/min). Results are presented in Figure S27a. DSC was performed on a DSC250 TA Instruments calorimeter. The samples were analyzed at a heating rate of 10 °C/min over a temperature range of −80 to 150 °C. Results are presented in Figure S27b. Tensile strength tests were performed with an Instron 5586 machine linked to the BlueHill software on sample rods (size = 8 mm × 10 mm × 0.08 mm) at room temperature at a rate of 2 mm/min.

Published in: Applied Materials & Interfaces (2021), vol. 13, pp. 54396–54408
DOI: 10.1021/acsami.1c16917
Status : Postprint (Author's version)

Modulus was determined by measuring the slope at the beginning of the curve. Results are presented in Figures 8 and S26.

RESULTS AND DISCUSSION

Scheme 1 illustrates the strategy used to develop high performance FA depolluting PHUs, as well as the structure of the different PHU precursors already validated for constructing PHU hydrogels.[59,60] As the properties of PHUs are notably dictated by the nature of their precursors, i.e., polycyclic carbonate and polyamine, we decided to evaluate the potential of these precursors to scavenge FA when taken alone. In a second step, the candidates presenting the highest capture ability will be selected to construct the depolluting PHU.

Scheme 1. Strategy for the Development of PHUs for FA Capture[a]

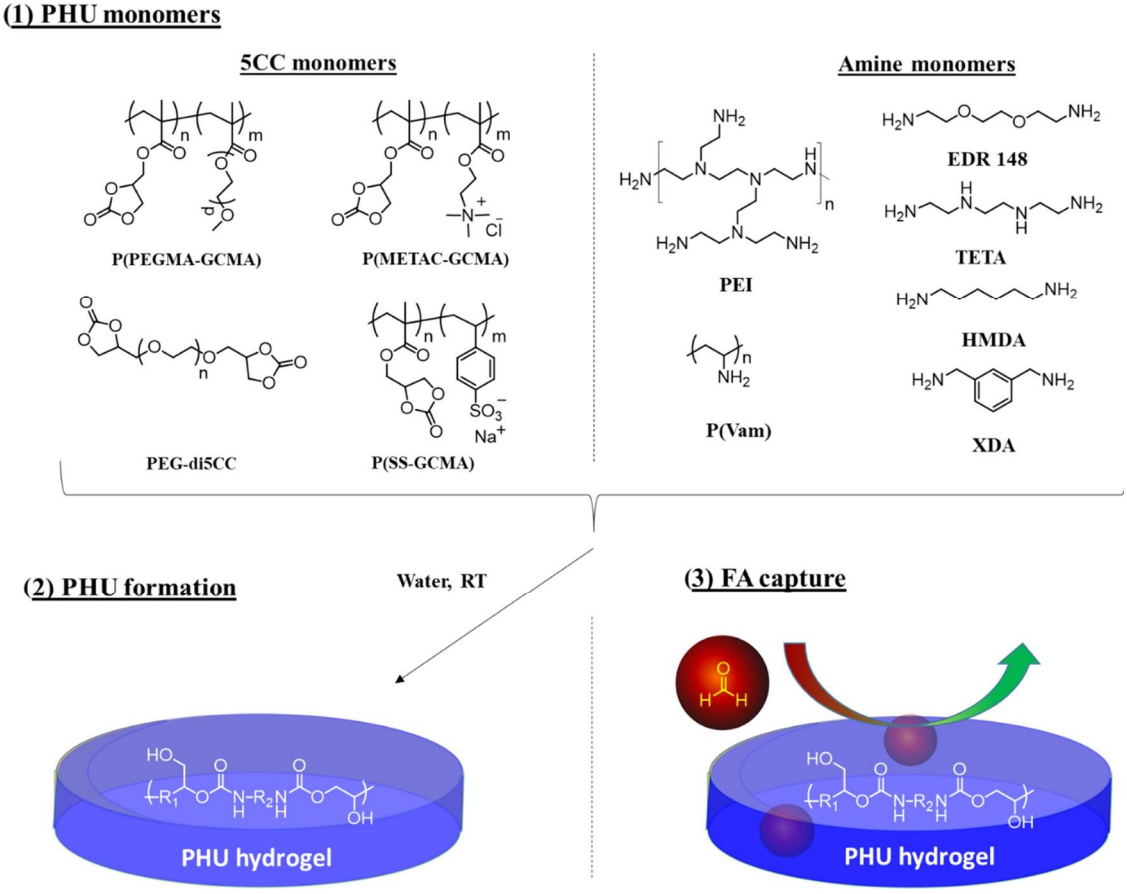

[a] (1) Selection of 5CC polymers and amine precursors for the formulation of PHUs with FA capture ability. (2) Formation of depolluting PHUs in water without organic solvent. (3) Formaldehyde capture by PHU hydrogel.

Published in: Applied Materials & Interfaces (2021), vol. 13, pp. 54396–54408
DOI: 10.1021/acsami.1c16917
Status : Postprint (Author's version)

FA Capture Potential of the PHU Precursors and Selection of the Most Relevant Candidates. The capture experiments were carried out at a fixed concentration of formaldehyde ([FA] = 1 mM) at room temperature (rt) in water. Free FA that did not interact or react with 5CCs bearing polymers or polyamines was titrated by the colorimetric NASH test according to a standard protocol that is detailed in the Experimental Section.

None of the 5CC polymers, whether cationic, anionic, or neutral, was efficient for capturing FA as illustrated in Figure S3 as only a negligible reduction of the FA concentration upon contact for 1 h at rt was noticed. This observation is correlated to the absence of appropriate chemical groups able to react with FA.

Importantly, all amines represented in Figure 1A were able to capture FA as expected, however with an impressive difference between poly(vinyl amine) (PVam) and all other tested amines. While at a pH of 10.5, almost 100% of FA was captured by PVam and triethylenetetramine (TETA) (when using a $[NH_2]/[FA]$ ratio of 500), less than 50% of FA was captured by the other amines (Figure 1B). Under identical conditions at pH 8.5, only PVam was able to capture 100% FA, with about 65% for TETA and less than 20% for the other amines (Figure 1C). The decrease in the performance of all amines (except for PVam) with pH reduction is in line with some reported studies performed on other amines.[3] The outstanding FA capture ability of PVam was better exemplified by decreasing the $[NH_2]/[FA]$ ratio from 500 to 50, with a complete FA adsorption by PVam, while the other amines were almost inactive (Figure 1D). Longer incubation times, from 1 to 4 h, did not improve the capture efficiency for these less active amines (Figure S4). PVam was also highly active at a much lower amine excess ($[NH_2]/[FA] = 5$), with more than 90% of captured FA in 1 h (Figure 1E). When using an equimolar content of amine groups and FA, about 37% of FA was still captured. Importantly, for the lower optimal $[NH_2]/[FA]$ ratio of 5, the PVam activity was almost similar regardless of the tested pH (3.5, 7.2, or 10.5) (Figure 1F). The yield of capture for a $[NH_2]/[FA]$ ratio of 1 was no more influenced by pH (Figure 1G).

The action mode of FA capture by PVam was studied by analyzing the reaction medium in D_2O by ^1H NMR spectroscopy at two different pHs (10.5 and 3.5) for the $[NH_2]/[FA]$ ratio of 5 ([FA] = 0.1M). Figure 2A shows the ^1H NMR of PVam at a pH of 10.5 with the characteristic resonances at 1.35 ppm for $-\underline{CH_2}-$ and at 2.95 ppm for $-\underline{CH}-NH_2$ of the polymer backbone. In the presence of FA (Figure 2B), new resonances appeared at 2.75 and 3.6 ppm corresponding to methylene bridges created from the reaction of FA with two adjacent amines, in line with observations also reported for other systems[61,62] and for PVam.[63]

Published in: Applied Materials & Interfaces (2021), vol. 13, pp. 54396–54408
DOI: 10.1021/acsami.1c16917
Status : Postprint (Author's version)

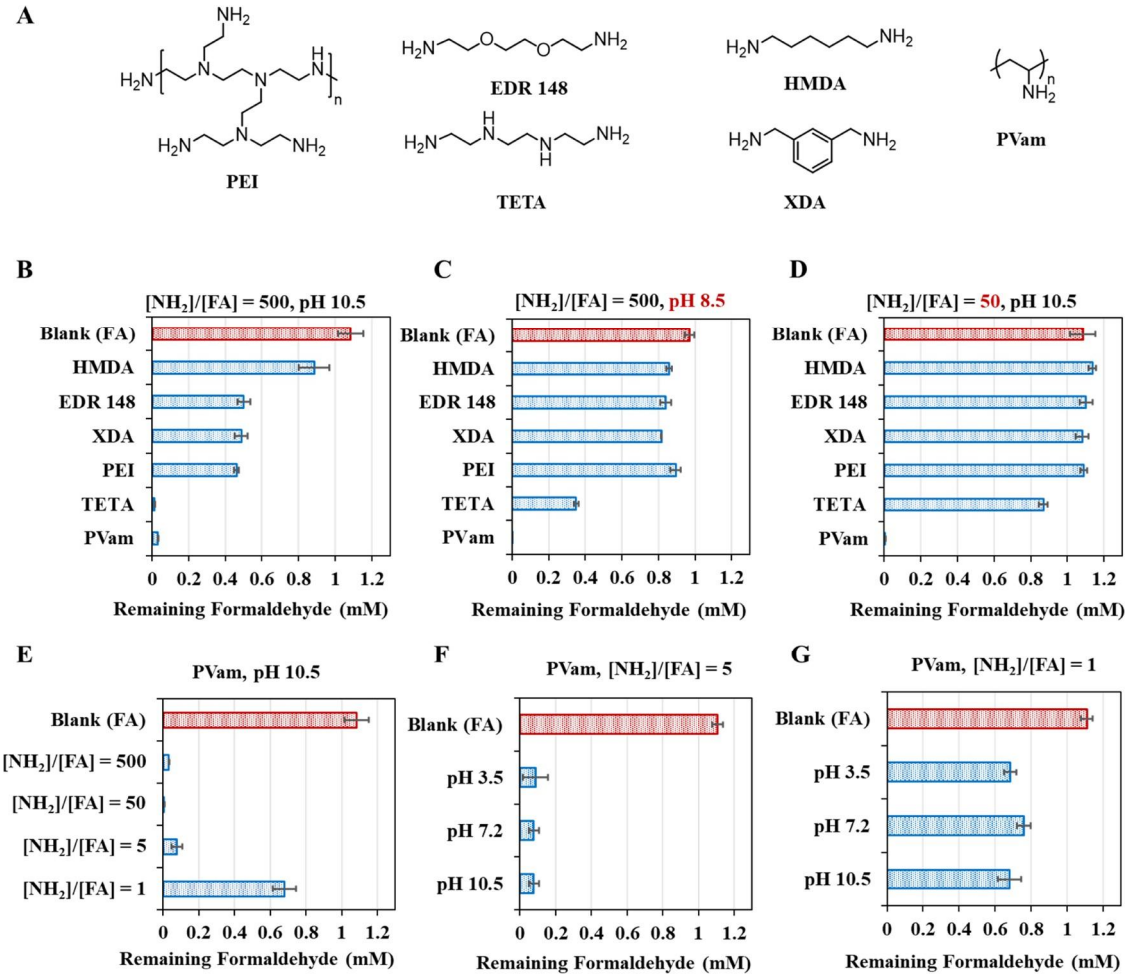

Figure 1. Formaldehyde capture experiments by various amines and under various conditions. (A) Structures of the different tested amines. FA capture efficiency by different amines (B) at pH = 10.5 for $[NH_2]/[FA]$ = 500, (C) at pH = 8.5 for $[NH_2]/[FA]$ = 500, and (D) at pH = 10.5 for $[NH_2]/[FA]$ = 50. (E) Influence of $[NH_2]/[FA]$ molar ratio on FA capture by PVam at pH = 10.5. (F) Influence of pH on FA capture by PVam for $[NH_2]/[FA]$ = 5. (G) Influence of pH on FA capture by PVam for $[NH_2]/[FA]$ = 1. Conditions: 1 h of incubation in water at rt, [FA] = 1 mM.

Published in: Applied Materials & Interfaces (2021), vol. 13, pp. 54396–54408
DOI: 10.1021/acsami.1c16917
Status : Postprint (Author's version)

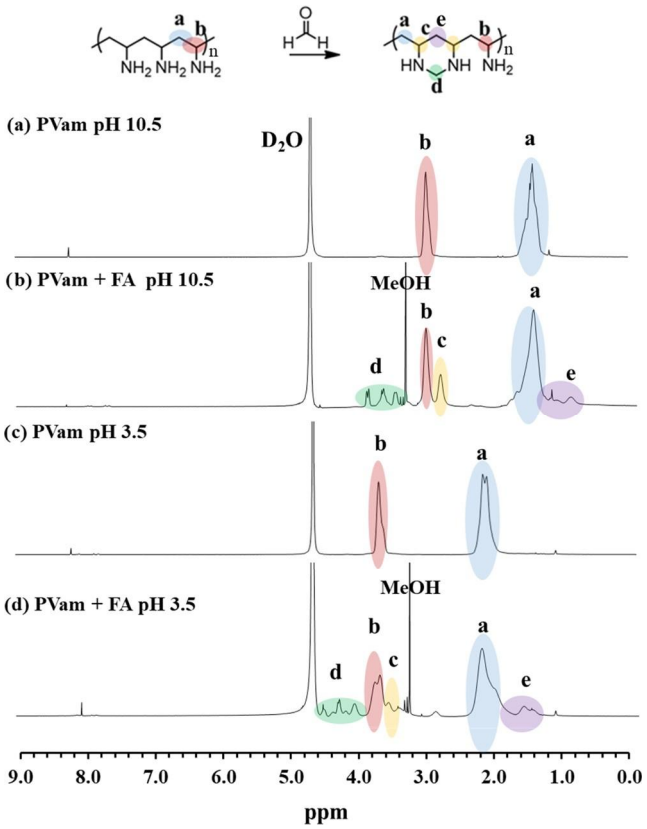

Figure 2. ^{1}H NMR spectra of (a) PVam at a pH of 10.5, (b) PVam + FA at a pH of 10.5, (c) PVam at a pH of 3.5, and (d) PVam + FA at a pH of 3.5. Conditions: RT, D_2O, $[NH_2]$ = 0.5 M, $[NH_2]/[FA]$ = 5, reaction time = 16 h (the resonance of methanol at 3.3 ppm results from methanol that is used as a FA stabilizer in the commercial FA aqueous solution).

With PVam, the driving force of the reaction relies on the formation of a six membered ring adduct.[63] These assignments were confirmed by HSQC and COSY experiments (Figure S5).

At pH 3.5, the resonances of PVam (without FA) were shifted downfield at 2.1 and 3.8 ppm due to the protonation of the amines (Figure 2C). In the presence of FA, the methylene bridges were also observed at higher values compared to the product formed at pH 10.5, also as the result of the protonation of the amines (Figure 2D). All assignments were also confirmed by HSQC and COSY experiments (Figure S6). This experiment clearly demonstrates that FA was reacting with PVam even when the amines were almost all protonated (protonation state > 90%[64]), confirming the excellent FA capture ability of PVam even under acidic conditions (Figure 1F). Quantification of the capture efficiency was realized via $_1$ H NMR spectroscopy. Based on the integration of protons c assigned to methylene bridges, 97% of FA has reacted with PVam at a pH of 10.5, supporting the remarkable potential of PVam for FA capture.

Synthesis of PHU Hydrogels with FA Capture Ability. To the best of our knowledge, PVam was never used to construct PHU hydrogels nor exploited for FA abatement applications. As PVam is highly soluble in water, the PHU hydrogels were prepared by the polyaddition of PVam to the hydrosoluble dicyclic carbonate (PEG-di5CC) in water (pH of 10) at rt under catalyst-free conditions as illustrated in

Published in: Applied Materials & Interfaces (2021), vol. 13, pp. 54396–54408
DOI: 10.1021/acsami.1c16917
Status : Postprint (Author's version)

Figure 3A. As an excess of NH_2 groups was required for FA capture, we investigated the influence of the [NH_2]/[5CC] ratio (from 1 to 7) on the properties of the PHU gel for a constant concentration in PHU (5 wt %). We have indeed to ensure that all PVam was chemically anchored to the polymer matrix to avoid its diffusion out of the hydrogel.

The curing of all formulations was followed by rheology by monitoring the time evolution of the storage (G') and loss (G'') moduli values and to determine the gel time (corresponding to the crossover point between G' and G'') (Figures 3B and S7). The transformation of the cyclic carbonate units into hydroxyurethane linkages was evidenced by infrared spectroscopy after 24 h of polymerization for the freeze-dried samples (Figure 3C). When an equimolar ratio between NH_2 and 5CC groups was used, no gelation was noted as no crossover between the storage modulus curve (G') and the loss modulus one (G'') was observed within 1 h of reaction (Figure 3B). The IR spectrum of the freeze-dried hydrogel obtained after 24 h of reaction indicated that only limited amounts of 5CCs were converted into hydroxyurethane linkages as attested by the slight decrease of the band at 1790 cm^{-1} (related to the carbonyl of 5CC) and the appearance of a low-intensity band at 1690 cm^{-1} related to the carbonyl of the urethane function (Figures 3C and S8). For a [NH_2]/[5CC] ratio of 2, a gel point was observed after 32 min of reaction (Figure 3B). However, G' values remained low, around 30 Pa after 2 h, indicating that the cross-linking density of the hydrogel was low. FT-ATR characterization corroborated the limited 5CC conversion after 24 h by the presence of an intense band at 1790 cm^{-1} (Figures 3C and S9). For [NH_2]/[5CC] = 4, an impressive short gel time of 2.5 min was noted, with a sharp and strong increase of G' till 1451 Pa, suggesting a highly cross-linked hydrogel (Figure 3B). After about 105 min of reaction, the G' value did not evolve further, which indicated that the reaction was finished, in line with the total consumption of the 5CC evidenced by FT-ATR with no visible residual carbonyl signal at 1790 cm^{-1} (Figures 3C and S10). When the [NH_2]/[5CC] ratio was further increased to 7, although a short gel time was noted (<1 min), G' values at the plateau were twice lower than that for the previous ratio of 4 (670 Pa vs 1451 Pa) (Figure 3B). This decrease was explained by the lower theoretical cross-linking density. Indeed, at a constant mass of solid content in hydrogel (5 wt %), a higher [NH_2]/[5CC] ratio corresponds to a lower concentration in 5CC and so lower hydroxyurethane crosslinks. Moreover, the very short pot life (<1 min) will render the future preparation and the application of the coating challenging. Therefore, a [NH_2]/[5CC] ratio of 4 was selected as the most appropriate for the formation of PHU hydrogels since it will guarantee a fast reaction with a high storage modulus. At this optimal ratio, we then evaluated the influence of pH on the hydrogel formation. Rheology measurements (Figure 3D) showed that gel time was considerably increased from 2.5 to 20 min when the pH was decreased from 10 to 8.5. The plateau in G' values was rapidly reached at pH 10 (90 min, suggesting that the reaction was complete), while it was not at a pH of 8.5 even after 5 h of reaction. After 24 h of polymerization, the FT-ATR spectra of the two hydrogels were similar and evidenced the complete disappearance of the carbonyl band representative of the 5CC moieties at 1790 cm^{-1} and the appearance of the urethane carbonyl signal at 1690 cm^{-1}, in line with the completeness of the reaction (Figure 3E). For a given [NH_2]/[5CC] ratio, the gel time (and thus the pot life of the formulation) can therefore be adjusted by simply modulating the pH of the reaction medium.

Published in: Applied Materials & Interfaces (2021), vol. 13, pp. 54396–54408
DOI: 10.1021/acsami.1c16917
Status : Postprint (Author's version)

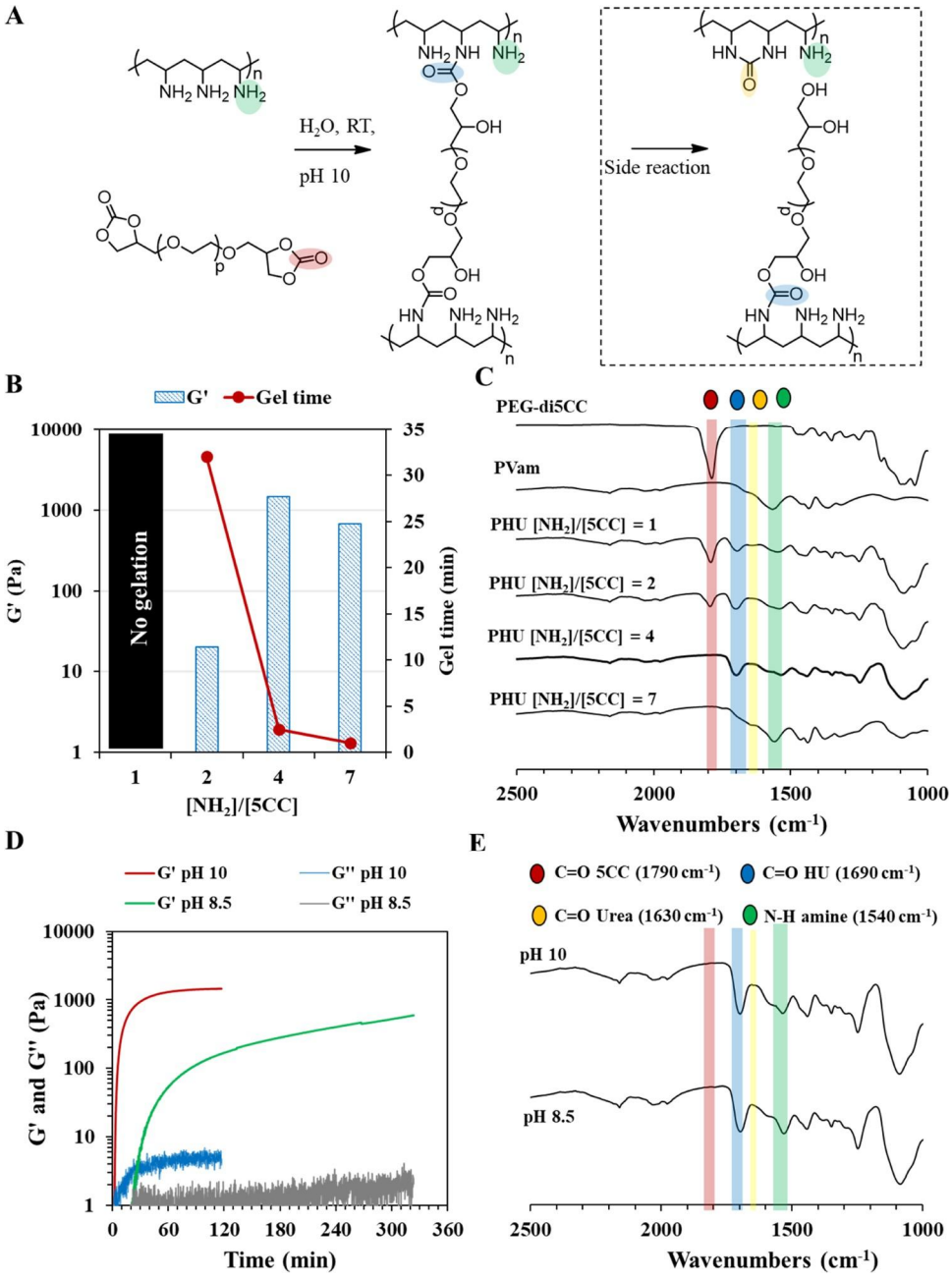

Figure 3. Formation of PHU hydrogels by polyaddition of PVam to PEG-di5CC. (A) Scheme of the reaction. (B) Storage modulus and gel times for PHU prepared with different $[NH_2]/[5CC]$ ratios at pH 10. (C) Infrared spectra of PHU hydrogels prepared from the different $[NH_2]/[5CC]$ ratios after 24 h at pH 10 (complete spectra are presented in Figures S8−S11). (D) Rheology experiments for the formation of PHU at different pHs with a constant $[NH_2]/[5CC]$ of 4. (E) Infrared spectra of PHU prepared with a $[NH_2]/[5CC]$ ratio of 4 after 24 h at pHs 8.5 and 10. Synthesis conditions: PHU 50 mg/mL in water at 25 °C.

Published in: Applied Materials & Interfaces (2021), vol. 13, pp. 54396–54408
DOI: 10.1021/acsami.1c16917
Status : Postprint (Author's version)

Besides the formation of hydroxyurethane linkages, we suspected a side reaction coming from the nucleophilic attack of an (adjacent) amine on the carbonyl group of hydroxyurethane leading to the formation of (cyclic) urea (Figure 3A) as already reported at the interface of the polycarbonate-PVam composite.[65] Urea linkages are characterized by a C=O elongation between 1600 and 1670 cm^{-1} in IR spectroscopy[65] and were detected by the presence of a band at 1630 cm^{-1} for $[NH_2]/[5CC] = 1$ and $[NH_2]/[5CC] = 7$ when the reaction occurred at pH 10 (Figures S8 and S11). This signal was more difficult to observe for $[NH_2]/[5CC] = 2$ and 4 (Figures S9 and S10) due to some overlapping with the HU band at 1690 $cm^{-1}$and the amine one at 1540 cm^{-1}.

To provide additional clues to the formation of this urea, the reaction of PVam with a low molar mass 5CC used as a model compound (i.e., ethylene carbonate, EC) was carried out in D_2O at pHs 8.5 and 10 at the optimal $[NH_2]/[5CC]$ ratio (i.e., $[NH_2]/[5CC] = 4$) (Figure 4A). The formation of urea was confirmed by IR with the presence of a peak at 1610 cm^{-1}, which was not found in native reagents (i.e., PVam and ethylene carbonate) or ethylene glycol formed by hydrolysis of EC (Figures 4C, S12, and S13). The polymer was also characterized by liquid-state ^1H NMR spectroscopy, and the proportion of the different adducts calculated after 8 h of reaction are presented in Figure 4D. The individual spectra before and after purification as well as the quantification by NMR spectroscopy are presented in Supporting Information (Figures S15 and S16 for pH 10 and Figures S17 and S18 for pH 8.5). First, the yield of urethane was slightly higher at pH 8.5 (24 mol %) in comparison to pH 10 (21 mol %). However, the total amount of functionalized amines was higher at pH 10 (40% vs 35% at pH 8.5), which indicated that a larger amount of urea was formed at pH 10 (19 mol % of the amines) than at pH 8.5 (11 mol % of the amines). It underlined that the nucleophilic substitution that transforms urethane into urea was influenced by the pH and was facilitated when amines were deprotonated.

Published in: Applied Materials & Interfaces (2021), vol. 13, pp. 54396–54408
DOI: 10.1021/acsami.1c16917
Status : Postprint (Author's version)

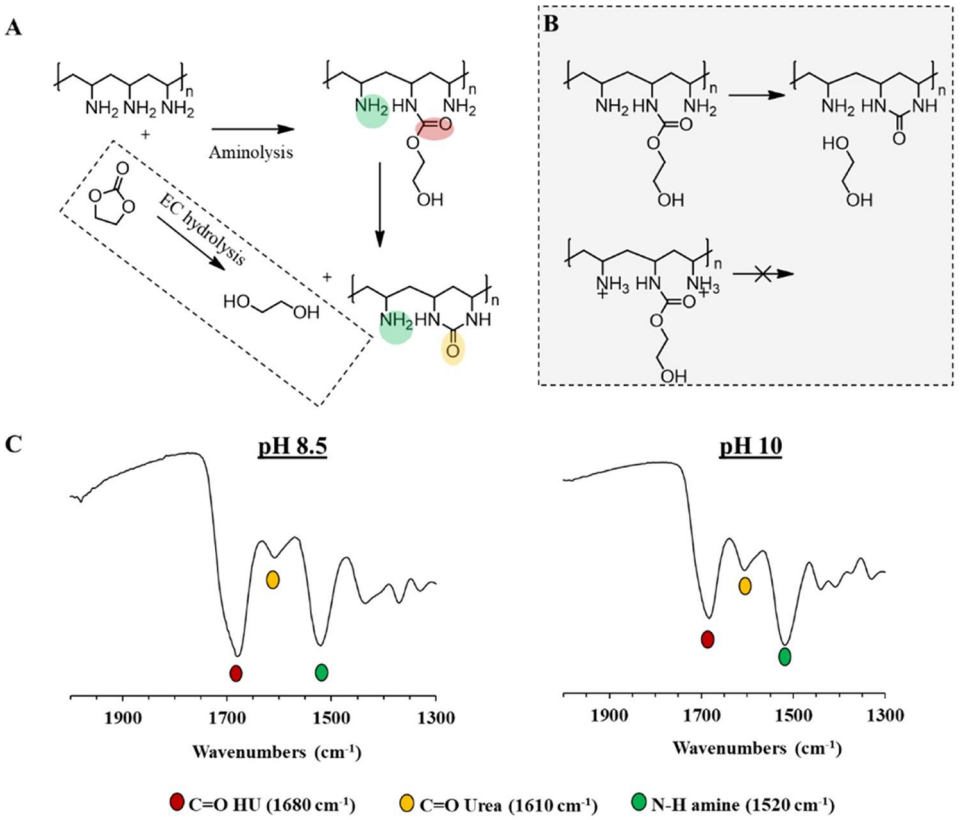

D

pH	$[NH_2]/[5CC]$	Polymer functionalization			Ethylene carbonate	
		Amine (%)	Urethane (%)	Urea (%)	Conv (%)	hydrolysis (%)
8.5	4	65	24	11	92	0
10	4	60	21	19	100	5

Figure 4. Characterization of the model reaction between PVam and EC in D_2O after 8 h of reaction. (A) Scheme of the different possible reactions in basic condition. (B) Proposed mechanism to explain the influence of pH. (C) Infrared spectra of purified products at pHs 8.5 and 10. (D) Table of conversion of amine of PVam into urethane or urea, and conversion or hydrolysis of EC at different pHs calculated by ^{1}H NMR (see Figures S15−S18 for complete spectra). Condition $[NH_2]$ = 0.4 M, D_2O, 8 h of reaction.

As reported earlier, when PHU hydrogels are prepared in water, some hydrolysis of 5CCs was noted, with a hydrolysis degree that increased with the pH of the reaction medium. This extent of hydrolysis was therefore quantified by calculating the content of ethylene glycol formed during hydrolysis at pHs of 8.5 and 10 (see the Supporting Information for details). We found that for $[NH_2]/[5CC]$ = 4, 5% of EC was hydrolyzed at a pH of 10 and 0% at a pH of 8.5, in line with other published results.[59]

Figure 5 illustrates the evolution of urethane/urea function conversion along time under the same conditions (i.e., $[NH_2]/[5CC]$ = 4 at pH 8.5 or 10, in water) according to ^{1}H NMR spectroscopy (Figure S19). At pH 10, the formation of urea largely increased during the first day of reaction and then increased to a lower but constant level for 3 weeks (Figure 5a). Besides, the amount of urethane linkages decreased, in line with the transformation of urethane into urea. At pH 8.5, the contents of urethane and urea rapidly stabilized between 1 and 5 days and kept constant for 3 weeks (Figure 5b).

Published in: Applied Materials & Interfaces (2021), vol. 13, pp. 54396–54408
DOI: 10.1021/acsami.1c16917
Status : Postprint (Author's version)

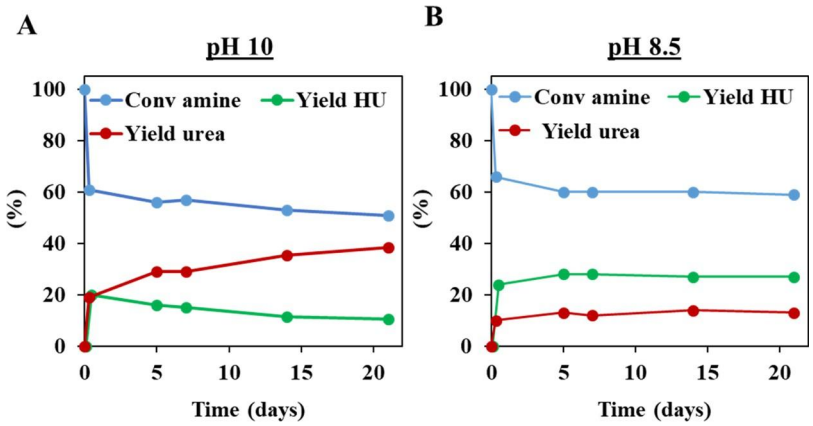

Figure 5. Evolution of amine, urethane, or urea groups with the time of reaction between PVam and EC calculated by ^{1}H NMR at (A) pH 10 and (B) pH 8.5. Conditions: RT, D_2O, $[NH_2]/[5CC] = 4$, and $[NH_2] = 0.4$ M.

These initial studies showed that pH influenced the urethane/urea formation under wet conditions. As the final target application of the hydrogels is coating in dried state under ambient condition, we followed the evolution of the hydrogel at the dried state by IR spectroscopy. The coatings were prepared from a fresh formulation of PEG-di5CC and PVam (5 wt %, $[NH_2]/[5CC] = 4$) at pH 10 and 8.5 and were dried at rt under ambient atmosphere. They were analyzed after 24 h and 7 days to identify any evolution of the polymer structure during aging (Figure S20). First, we observed that remaining 5CC characterized by a band at 1790 cm^{-1} was more important at pH 8.5 than 10 after 24 h of drying (Figure S20a). However, signal corresponding to the hydroxyurethane linkages (HU) at 1690 cm^{-1} had the same intensity at both pHs. A small band assigned to urea at 1630 cm^{-1} was also observed in all spectra. All 5CCs were consumed at both pHs after 7 days. It was noted that between 24 h and 7 days, no evolution of HU band at 1690 cm^{-1} and urea band at 1630 cm^{-1} was observed at both pHs of 10 and 8.5, indicating that under dried conditions, the transformation of urethane to urea was less prone to happen than in solution (Figure S20).

Ability of PHU Hydrogels for Formaldehyde Capturing in Water. Capitalizing on our optimization study, the most promising PHU hydrogel for FA capturing (Figure 6A) was prepared with an amine excess ($[NH_2]/[5CC] = 4$) at rt for 24 h. The pH was fixed to 10 to promote a short gel time and to limit the content of unreacted 5CCs within the network. After 24 h of reaction, a FA solution was added on the PHU hydrogel and the quantification of free FA by the NASH test was monitored over time to evaluate the ability of PHU to FA capturing (see the Experimental Section). The evolution of the FA concentration in contact with PHU was compared to a solution of FA that did not contain PHU (Figure 6B). This figure shows a rapid decrease in the FA concentration from 1 to 0.14 mM in the presence of PHU, which corresponded to an impressive FA abatement of 86% within 1 h. When the concentration of FA was increased to 10 mM (thus with a ratio $[NH_2]/[FA] = 10$), we observed an abatement of 70% of FA after 1 h, further highlighting the ability of the hydrogel to capture FA. During these experiments, an important swelling of the PHU hydrogel was noted when immersed in water, i.e., around 1800% after 1 h and 7000% after 24 h. Importantly, there was no significant difference in the swelling of the

Published in: Applied Materials & Interfaces (2021), vol. 13, pp. 54396–54408
DOI: 10.1021/acsami.1c16917
Status : Postprint (Author's version)

hydrogel in water in the presence or absence of FA (regardless of its concentration, 1 or 10 mM) as illustrated in Figure S21a. To evaluate the robustness of the process, we also assessed the FA capture ability of the PHU hydrogel in the presence of some inorganic salts (NaCl, $CaCl_2$, Na_3PO_4) in the solution containing FA. Although NaCl and $CaCl_2$ (both at 50 mM) were slowing down the FA capture after 1 h (61 and 63% of FA captured, respectively), Na_3PO_4 had almost no influence (82% of capture vs 86% without this salt) (Figure S22). These results were correlated to the lower swelling of the hydrogel in saline solution in comparison to water (2.6-fold lower for NaCl or $CaCl_2$, and 1.6-fold lower for Na_3PO_4 in comparison to water; Figure S21b). The rate of diffusion of FA was thus expected to be reduced in the less swollen hydrogels containing NaCl or $CaCl_2$. After 24 h exposure, all hydrogels presented a similar and high FA abatement (> 90%). Conclusively, salts that were decreasing the swelling of the hydrogel were reducing the rate of diffusion of FA inside PHU but did not inhibit its FA capture ability nor the content of FA that can be scavenged for long contact times.

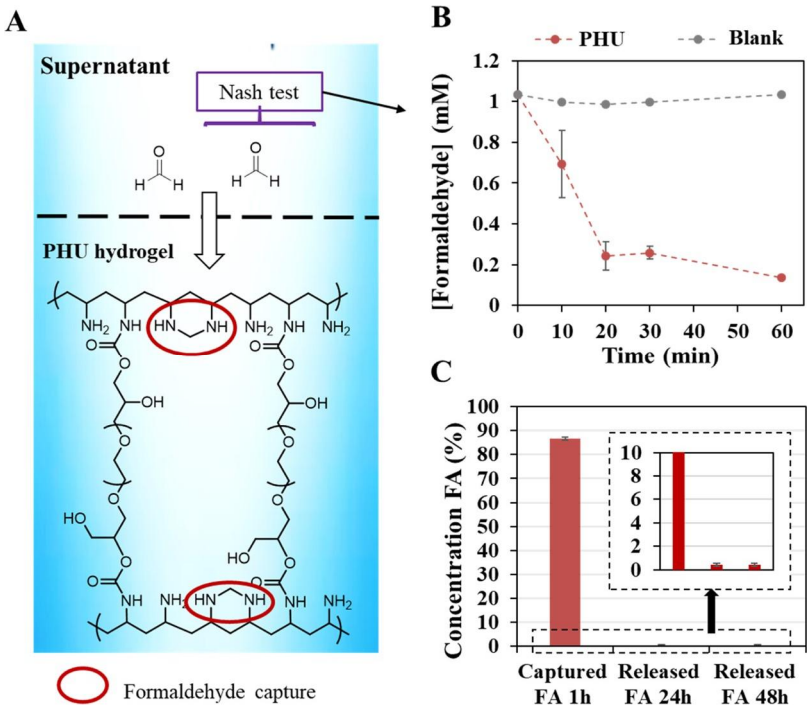

Figure 6. Formaldehyde removal in solution by PHU at 25 °C for $[NH_2]/[FA] = 100$. (A) Scheme of FA capture by PHU. (B) Evolution of FA concentration with time evaluated by the NASH test (conditions: PHU 5 wt %, $[NH_2]/[5CC] = 4$, pH 10, water, rt, FA 1 mM, $[NH_2]/[FA] = 100$). (C) Released FA after immersion of the hydrogels for 24 and 48 h in water at 25 °C (conditions: PHU 5 wt %, $[NH_2]/[5CC] = 4$, pH 10, water, rt, immersed first in 1mL of FA 1 mM and then in 1 mL of water at rt).

We then evaluated whether FA captured by PHU could be released over time. The hydrogel was thus immersed in water and released FA was quantified by the NASH test after 24 and 48 h. Figure 6C shows that less than 2% FA were released after 24 and 48 h of immersion, in agreement with the formation of a stable covalent adduct between FA and PHU (Figure 6A). These experiments demonstrate that the

Published in: Applied Materials & Interfaces (2021), vol. 13, pp. 54396–54408
DOI: 10.1021/acsami.1c16917
Status : Postprint (Author's version)

PHU hydrogel drastically reduced the concentration of FA in solution by a strong and permanent capture process.

PHU Coatings for Gaseous Formaldehyde Capturing and Indoor Air Purification. Although PHU hydrogels were able to capture FA in solution (thus at the hydrated state), their ability to scavenge gaseous FA when deposited as coatings (i.e., at the dried state) is unknown. For real-life applications, the performance of these PHU coatings for indoor air depollution has thus to be evaluated. For that purpose, the PHU ([NH_2]/[5CC] = 4) coating was prepared by depositing an aqueous solution of a mixture of PEG-di5CC (33 mg/mL) and PVam (17 mg/mL) on a stainless steel substrate by a bar coater (10 g of PHU/m^2) and was then dried under ambient atmosphere at rt for 24 h. The capacity of the coating to capture FA was then evaluated using a standardized procedure adapted from EN717-3,[58] detailed in the Experimental Section and illustrated in Figure 7A. In brief, the coated substrate was placed in a closed and hermetic plastic container that contained a FA emission vial ([FA] = 10 mM) and a water reception vial (Figure 7A). Emitted FA was thus interacting with the coating and solubilized in the reception vial. The more captured FA by the coating, the less FA was solubilized in the reception vial. The FA concentration in the reception vial was then assessed according to the colorimetric Nash test. The depolluting performance of PHU coating was compared to the nude stainless steel substrate used as a control. The experiment was carried out for 16 days. At each FA quantification, the reception vial was cleaned and the emission vial was refilled with FA at the same initial concentration ([FA] = 10mM).

Figure 7B shows an impressive decrease of FA concentration when using the substrate coated by PHU after 24 h only. This FA abatement was of 94% for PHU in comparison to nude stainless steel. The same observation was made after second and third days of exposure of the same coatings after adding a new fresh feed of FA for the new testing. This experiment evidenced that the PHU coating was not saturated by FA after the first and second tests and was thus able to further react with FA. Leaving these coated substrates for a longer period of time up to 16 days showed that the PHU coating was still highly active (the coated substrate was not changed before recharging the emission vial by FA), highlighting a remarkable capture capability for gaseous FA.

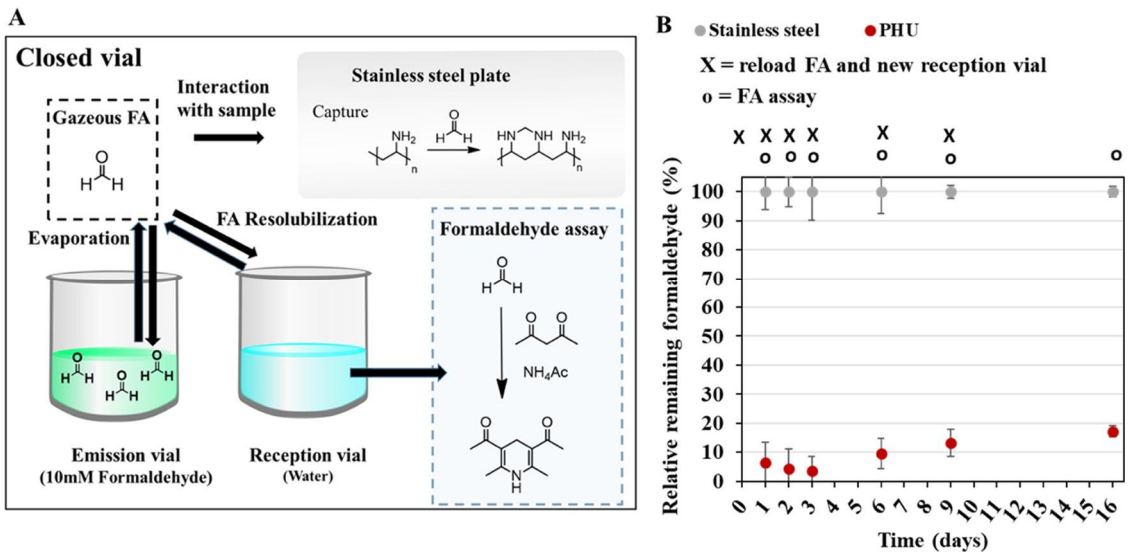

Published in: Applied Materials & Interfaces (2021), vol. 13, pp. 54396–54408
DOI: 10.1021/acsami.1c16917
Status : Postprint (Author's version)

Figure 7. Gaseous formaldehyde capture by PHU coated on stainless steel plates. (A) Scheme of the gaseous FA assay. (B) Results normalized to nude stainless steel (blank). Condition: 5 wt % precursor in water at rt, $[NH_2]/[5CC] = 4$, 10 g of PHU/m^2.

We then studied whether the loaded PHU obtained after 16 days of FA exposure was releasing FA over time at room temperature. Figure S23b does not show any release of FA from the PHU coating. A similar experiment was conducted at 40°C for 24 h, as this procedure was used by others to evaluate under accelerated conditions the desorption of physically adsorbed FA in wood-based panels.[2] Negligible FA release was also observed (Figure S24), in agreement with the permanent capture of FA in the PHU coating.

Mechanical and Thermal Properties, as well as Visual Aspect of PHU Films. We then evaluated the influence of the fixation of FA onto PHU on the mechanical properties of the PHU coating. The mechanical properties of the films were evaluated by measuring the tensile properties of the dried PHU films (thickness = 80 μm). The FA-loaded films were obtained by immersing the film in a solution of FA (1 mM with $[NH_2]/[FA] = 100$ or 10 mM with $[NH_2]/[FA] = 10$; see the Experimental Section for details).

Stress–strain curves of the different films are illustrated in Figure S26, and Young's modulus, stress at break, and strain at break values are summarized in Figure 8. The Young's modulus decreased from 137 MPa for pristine PHU to 87 and 40 MPa for PHU loaded by FA 1 and 10 mM, respectively (Figure 8A), while the stress at break remained in the same range for all samples (4.6–6 MPa; Figure 8B). Importantly, strain at break remained high (~325%) for PHU loaded with FA and higher than that for pristine PHU (Figure 8C). It can therefore be concluded that FA affected the mechanical properties of the PHU film that changed from a tough plastic-like material to a more elastomeric-like one, which is not deleterious for the target application as the film is able to accommodate more deformation after FA fixation.

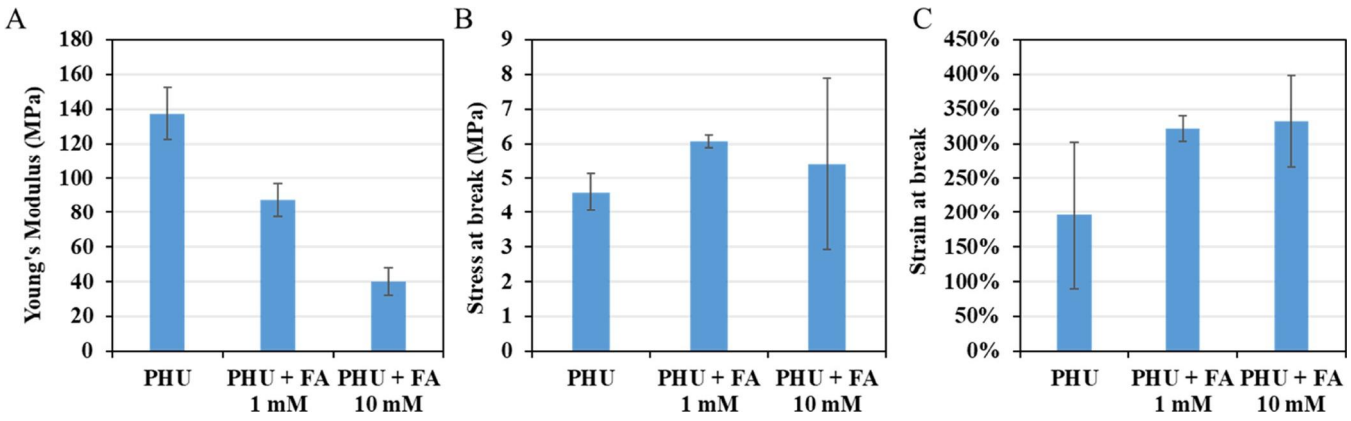

Figure 8. Tensile properties of dried PHU film before and after FA capture. (A) Young's modulus, (B) stress at break, and (C) strain at break. Condition: PHU film 5 wt %, $[NH_2]/[5CC] = 4$, at pH 10 for 48 h. Incubation in FA 1 mM ($[NH_2]/[FA] = 100$) or 10 mM ($[NH_2]/[FA] = 10$) for 1 h.

Published in: Applied Materials & Interfaces (2021), vol. 13, pp. 54396–54408
DOI: 10.1021/acsami.1c16917
Status : Postprint (Author's version)

Then, the thermal properties of PHU films loaded or not with FA were investigated. Thermogravimetric analysis (TGA) presented in Figure S27a showed similar thermograms between the different films, indicating that FA did not significantly affect the thermal stability behavior of PHU (at least in the FA loading range investigated in this study). It has to be noted that the first decrease in mass at a low temperature (10% of mass loss between 60 and 140 °C) was imparted to water evaporation from the highly hydrophilic coating stored under ambient condition after drying under air. The degradation temperature of these PHUs was high (T_d > 265 °C), in the same range as the ones measured for other more hydrophobic PHUs used as coatings.[66,67]

The glass-transition temperature of the films was also very similar whether they were unloaded (T_g = −39 °C) or loaded by FA (T_g = −34 °C), and no crystallization/melting transition was observed, proving the amorphous nature of the PHU films (Figure S27b).

Scanning electron microscopy of PHU loaded with FA (10 mM) did not show any cracks; a slight structuration of the film was however observed in comparison to pristine PHU (Figure S28). Although further investigation would be required to explain the reason for such structuration, the film remained perfectly transparent and colorless after FA capture (Figure 9).

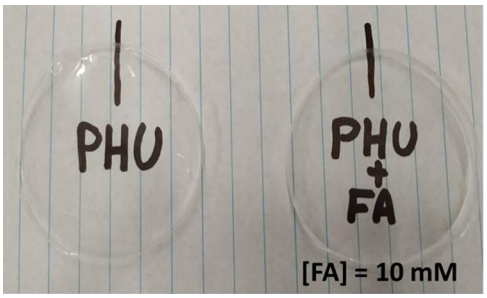

Figure 9. Images of PHU and PHU + FA (10 mM) films (thickness = 80 μm).

It is important to note that our colorless PHU films contrast to most of PHU films/coatings of the literature that are yellowish to brown.[67,68] This difference in coloration is the result of the processing of our films that occurred at room temperature, in comparison to elevated temperatures in the state-of-the-art developments that lead to the occurrence of side reactions responsible for yellowing.[69]

CONCLUSIONS

Although amines are often considered as good scavenging agents for formaldehyde (FA), the structural difference between them can largely influence their FA scavenging ability. This work showed that, in contrast to common polyamines, poly(vinyl amine) (PVam) presented outstanding capture ability for FA in a large range of concentrations and pHs, with the formation of methylene bridges between two amines by reaction with FA. The incorporation of PVam in material design for FA abatement appeared thus an evidence. We thus reported the synthesis of PHU hydrogels for FA capture by the polyaddition of a hydrophilic poly(cyclic carbonate) (polyethylene glycol bearing a cyclic carbonate at both ends) to PVam in water at room temperature. Without any catalyst, short gel times were noted (2 min) at a pH

of 10 when an excess of amines was used ([NH_2]/[5CC] = 4), and the reaction was complete within 2 h. Based on model reactions, this amine excess was found to be optimal for FA capture, while enabling the formation of PHU hydrogels. Some side reactions within the PHU network were observed when the hydrogel was maintained in wet state at a pH of 10, due to the transformation of some urethane linkages into urea ones. Decreasing this pH to 8.5 strongly limited this side reaction. Importantly, when PHU was processed as a coating and dried under ambient conditions, this side reaction did not occur. The FA capture performance of amine-functionalized PHU was then evaluated in solution and showed an impressive FA abatement without any significant release of FA after scavenging in line with its covalent and permanent grafting to PHU. We have also processed this PHU as a coating on a stainless steel substrate, and it displayed high FA scavenging ability over a long period of time, without noticeable saturation. The preparation of the PHU formulation is straightforward in water at room temperature without using any catalyst, and its pot life can be easily tuned by adapting the pH of the solution. The PHU coatings are transparent and colorless, even after FA capture. As the formulations can potentially be deposited on various surfaces of our living spaces (wall, ceiling, furniture, etc.), this work demonstrates that coatings made of poly(vinyl amine)-based PHUs are highly promising for providing sustainable solutions for depolluting indoor air from toxic formaldehyde.

Supporting Information

The Supporting Information is available free of charge at https://pubs.acs.org/doi/10.1021/acsami.1c16917.

Materials description; characterization tools; ^{1}H, ^{13}C, HSQC, COSY NMR spectra, and ATR characterizations; complementary results on formaldehyde capture by 5CC precursors; and synthesis procedures for polyvinylamine and five-membered cyclic carbonate monomers (PDF)

Author Contributions

The manuscript was written through contributions of all authors. All authors have given approval to the final version of the manuscript.

Notes

The authors declare no competing financial interest.

ACKNOWLEDGMENTS

This research was financed by "le Fonds européen de développement régional (FEDER) et la Wallonie dans le cadre du programme opérationnel 'Wallonie-2020.EU'" in the frame of the BIODEC project. C.D. and B.G. thank the "Fonds National pour la Recherche Scientifique" (F.R.S.-FNRS) and the Fonds Wetenschappelijk Onderzoek Vlaanderen (FWO) for financial support in the frame of the Excellence of Science (EOS) project no. O019618F (ID EOS: 30902231). C.D. is Research Director of F.R.S-FNRS.

REFERENCES

(1) Tang, X.; Bai, Y.; Duong, A.; Smith, M. T.; Li, L.; Zhang, L. Formaldehyde in China: Production, Consumption, Exposure Levels, and Health Effects. Environ. Int. 2009, 35, 1210–1224.

(2) Salthammer, T.; Mentese, S.; Marutzky, R. Formaldehyde in the Indoor Environment. Chem. Rev. 2010, 110, 2536–2572.

(3) Kamps, J. J. A. G.; Hopkinson, R. J.; Schofield, C. J.; Claridge, T. D. W. How Formaldehyde Reacts with Amino Acids. Commun. Chem., 2019, 2, No. 126.

(4) WHO. Air Quality Guidelines for Europe, 2000.

(5) Al-Rashid, J.; Adamczyk, A.; Panitzsch, T.; Lal, G.; Arnold, A.; Su, J. Aldehyde Emissions from Flexible Molded Foam, 2015.

(6) Ghani, A.; Ashaari, Z.; Bawon, P.; Lee, S. H. Reducing Formaldehyde Emission of Urea Formaldehyde-Bonded Particleboard by Addition of Amines as Formaldehyde Scavenger. Build. Environ. 2018, 142, 188–194.

(7) Xuechuan, W.; Longfang, R.; Taotao, Q. Novel Way of Transformation of Tannery Waste to Environmentally Friendly Formaldehyde Scavenger. Environ. Prog. Sustainable Energy 2009, 28, 285–290.

(8) Hoong, Y. B.; Paridah, M. T.; Loh, Y. F.; Koh, M. P.; Luqman, C. A.; Zaidon, A. Acacia Mangium Tannin as Formaldehyde Scavenger for Low Molecular Weight Phenol-Formaldehyde Resin in Bonding Tropical Plywood. J. Adhes. Sci. Technol. 2010, 24, 1653–1664.

(9) Barbu, M. C.; Lohninger, Y.; Hofmann, S.; Kain, G.; Petutschnigg, A.; Tudor, E. M. Larch Bark as a Formaldehyde Scavenger in Thermal Insulation Panels. Polymers 2020, 12, No. 2632.

(10) Boran, S.; Usta, M.; Ondaral, S.; Gümüskaya, Ę . The Efficiency of Tannin as a Formaldehyde Scavenger Chemical in Medium Density Fiberboard. Composites, Part B 2012, 43, 2487–2491.

(11) Liu, Y.; Qin, X.; Zhu, X.; Wu, L.; Xu, Y.; Huang, K.; Huang, J.; Chen, Y. Microencapsulation of Formaldehyde Scavenger Agent and Its Application to Veneered Panels. Eur. J. Wood Prod. 2021, 79, 579– 588.

(12) Costa, N. A.; Pereira, J.; Ferra, J.; Cruz, P.; Martins, J.; Magalhaes̃, F. D.; Mendes, A.; Carvalho, L. H. Scavengers for Achieving Zero Formaldehyde Emission of Wood-Based Panels. Wood Sci. Technol. 2013, 47, 1261–1272.

(13) de Cademartori, P. H. G.; Artner, M. A.; Alves de Freitas, R.; Magalhães, W. L. E. Alumina Nanoparticles as Formaldehyde Scavenger for Urea-Formaldehyde Resin: Rheological and in-Situ Cure Performance. Composites, Part B 2019, 176, No. 107281.

(14) Robert, B.; Nallathambi, G. Indoor Formaldehyde Removal by Catalytic Oxidation, Adsorption and Nanofibrous Membranes: A Review. Environ. Chem. Lett. 2021, 19, 2551–2579.

(15) Quiroz Torres, J.; Royer, S.; Bellat, J.-P.; Giraudon, J.-M.; Lamonier, J.-F. Formaldehyde: Catalytic Oxidation as a Promising Soft Way of Elimination. ChemSusChem 2013, 6, 578–592.

Published in: Applied Materials & Interfaces (2021), vol. 13, pp. 54396–54408
DOI: 10.1021/acsami.1c16917
Status : Postprint (Author's version)

(16) Zhang, Y.; Xiong, G.; Yao, N.; Yang, W.; Fu, X. Preparation of Titania-Based Catalysts for Formaldehyde Photocatalytic Oxidation from TiCl4 by the Sol–Gel Method. Catal. Today 2001, 68, 89–95.

(17) Portela, R.; Jansson, I.; Suárez, S.; Villarroel, M.; Sánchez, B.; Avila, P. Natural Silicate-TiO2 Hybrids for Photocatalytic Oxidation of Formaldehyde in Gas Phase. Chem. Eng. J. 2017, 310, 560–570.

(18) Liu, H.; Ye, X.; Lian, Z.; Wen, Y.; Shangguan, W. Experimental Study of Photocatalytic Oxidation of Formaldehyde and Its ByProducts. Res. Chem. Intermed. 2006, 32, 9–16.

(19) Chen, M.; Wang, H.; Chen, X.; Wang, F.; Qin, X.; Zhang, C.; He, H. High-Performance of Cu-TiO2 for Photocatalytic Oxidation of Formaldehyde under Visible Light and the Mechanism Study. Chem. Eng. J. 2020, 390, No. 124481.

(20) Zhu, X.; Jin, C.; Li, X.-S.; Liu, J.-L.; Sun, Z.-G.; Shi, C.; Li, X.; Zhu, A.-M. Photocatalytic Formaldehyde Oxidation over Plasmonic Au/TiO2 under Visible Light: Moisture Indispensability and Light Enhancement. ACS Catal. 2017, 7, 6514–6524.

(21) Sun, S.; Ding, J.; Bao, J.; Gao, C.; Qi, Z.; Li, C. Photocatalytic Oxidation of Gaseous Formaldehyde on TiO2: An In Situ DRIFTS Study. Catal. Lett. 2010, 137, 239–246.

(22) Guo, J.; Lin, C.; Jiang, C.; Zhang, P. Review on Noble MetalBased Catalysts for Formaldehyde Oxidation at Room Temperature. Appl. Surf. Sci. 2019, 475, 237–255.

(23) Zhang, C.; He, H.; Tanaka, K. Catalytic Performance and Mechanism of a Pt/TiO2 Catalyst for the Oxidation of Formaldehyde at Room Temperature. Appl. Catal., B 2006, 65, 37–43.

(24) Zhang, C.; He, H. A Comparative Study of TiO2 Supported Noble Metal Catalysts for the Oxidation of Formaldehyde at Room Temperature. Catal. Today 2007, 126, 345–350.

(25) Zhang, C.; He, H.; Tanaka, K. Perfect Catalytic Oxidation of Formaldehyde over a Pt/TiO2 Catalyst at Room Temperature. Catal. Commun. 2005, 6, 211–214.

(26) Cai, T.; Zhang, P.; Shen, X.; Huang, E.; Shen, X.; Shi, J.; Wang, Z.; Sun, Q. Synthesis of Pt-Loaded NiFe-LDH Nanosheets on Wood Veneer for Efficient Gaseous Formaldehyde Degradation. ACS Appl. Mater. Interfaces 2020, 12, 37147–37154.

(27) Salthammer, T.; Fuhrmann, F. Photocatalytic Surface Reactions on Indoor Wall Paint. Environ. Sci. Technol 2007, 41, 6573–6578.

(28) Rezaei, M.; Fazlzadehdavil, M.; Hajizadeh, Y. Formaldehyde Removal from Airstreams Using a Biofilter with a Mixture of Compost and Woodchips Medium. Water, Air, Soil Pollut. 2015, 226, No. 2242.

(29) Yu, D.; Song, L.; Wang, W.; Guo, C. Isolation and Characterization of Formaldehyde-Degrading Fungi and Its Formaldehyde Metabolism. Environ. Sci. Pollut. Res. 2014, 21, 6016–6024.

(30) Asgher, M.; Yasmeen, Q.; Iqbal, H. M. N. Development of Novel Enzymatic Bioremediation Process for Textile Industry Effluents through Response Surface Methodology. Ecol. Eng. 2014, 63, 1–11.

(31) Zvulunov, Y.; Ben-Barak-Zelas, Z.; Fishman, A.; Radian, A. A Self-Regenerating Clay-Polymer-Bacteria Composite for Formaldehyde Removal from Water. Chem. Eng. J. 2019, 374, 1275–1285.

(32) Yamaguchi, M.; Tahara, Y.; Kanemaru, M.; Deguchi, M.; Ozawa, S.; Arar, J. In Formaldehyde Degradation Filter via Recombinant E. coli Enzyme, IEEE EMBS Asian-Pacific Conference on Biomedical Engineering, 2003; pp 106–107.

(33) Carter, E. M.; Katz, L. E.; Speitel, G. E.; Ramirez, D. Gas-Phase Formaldehyde Adsorption Isotherm Studies on Activated Carbon: Correlations of Adsorption Capacity to Surface Functional Group Density. Environ. Sci. Technol. 2011, 45, 6498–6503.

(34) Ma, C.; Li, X.; Zhu, T. Removal of Low-Concentration Formaldehyde in Air by Adsorption on Activated Carbon Modified by Hexamethylene Diamine. Carbon 2011, 49, 2873–2875.

(35) de Falco, G.; Li, W.; Cimino, S.; Bandosz, T. J. Role of Sulfur and Nitrogen Surface Groups in Adsorption of Formaldehyde on Nanoporous Carbons. Carbon 2018, 138, 283–291.

(36) Baur, G. B.; Spring, J.; Kiwi-Minsker, L. Amine Functionalized Activated Carbon Fibers as Effective Structured Adsorbents for Formaldehyde Removal. Adsorption 2018, 24, 725–732.

(37) Tanada, S.; Kawasaki, N.; Nakamura, T.; Araki, M.; Isomura, M. Removal of Formaldehyde by Activated Carbons Containing Amino Groups. J. Colloid Interface Sci. 1999, 214, 106–108.

(38) Rengga, W. D. P.; Sudibandriyo, M.; Nasikin, M. Adsorption of Low-Concentration Formaldehyde from Air by Silver and Copper Nano-Particles Attached on Bamboo-Based Activated Carbon. Int. J. Chem. Eng. Appl. 2013, 4, 332–336.

(39) Li, J.; Li, Z.; Liu, B.; Xia, Q.; Xi, H. Effect of Relative Humidity on Adsorption of Formaldehyde on Modified Activated Carbons. Chinese J. Chem. Eng. 2008, 16, 871–875.

(40) Pei, J.; Zhang, J. S. On the Performance and Mechanisms of Formaldehyde Removal by Chemi-Sorbents. Chem. Eng. J. 2011, 167, 59–66.

(41) de Falco, G.; Barczak, M.; Montagnaro, F.; Bandosz, T. J. A New Generation of Surface Active Carbon Textiles As Reactive Adsorbents of Indoor Formaldehyde. ACS Appl. Mater. Interfaces 2018, 10, 8066–8076.

(42) Bellat, J.-P.; Bezverkhyy, I.; Weber, G.; Royer, S.; Averlant, R.; Giraudon, J.-M.; Lamonier, J.-F. Capture of Formaldehyde by Adsorption on Nanoporous Materials. J. Hazard. Mater. 2015, 300, 711–717.

(43) Nomura, A.; Jones, C. W. Enhanced Formaldehyde-Vapor Adsorption Capacity of Polymeric Amine-Incorporated Aminosilicas. Chem. - Eur. J 2014, 20, 6381–6390.

(44) Srisuda, S.; Virote, B. Adsorption of Formaldehyde Vapor by Amine-Functionalized Mesoporous Silica Materials. J. Environ. Sci. 2008, 20, 379–384.

(45) Nakayama, H.; Hayashi, A.; Eguchi, T.; Nakamura, N.; Tsuhako, M. Adsorption of Formaldehyde by Polyamine-Intercalated α-Zirconium Phosphate. Solid State Sci. 2002, 4, 1067–1070.

(46) Matsuo, Y.; Nishino, Y.; Fukutsuka, T.; Sugie, Y. Removal of Formaldehyde from Gas Phase by Silylated Graphite Oxide Containing Amino Groups. Carbon 2008, 46, 1162–1163.

(47) Song, S.; Song, A.; Feng, L.; Wei, G.; Dong, S.; Hao, J. Fluorescent Hydrogels with Tunable Nanostructure and Viscoelasticity for Formaldehyde Removal. ACS Appl. Mater. Interfaces 2014, 6, 18319−18328.

(48) hang, L.; Song, X.; Wu, J.; Long, C.; Li, A.; Zhang, Q. Preparation and Characterization of Micro-Mesoporous Hypercrosslinked Polymeric Adsorbent and Its Application for the Removal of VOCs. Chem. Eng. J. 2012, 192, 8−12.

(49) Long, C.; Liu, P.; Li, Y.; Li, A.; Zhang, Q. Characterization of Hydrophobic Hypercrosslinked Polymer as an Adsorbent for Removal of Chlorinated Volatile Organic Compounds. Environ. Sci. Technol. 2011, 45, 4506−4512.

(50) Long, C.; Li, Y.; Yu, W.; Li, A. Removal of Benzene and Methyl Ethyl Ketone Vapor: Comparison of Hypercrosslinked Polymeric Adsorbent with Activated Carbon. J. Hazard. Mater. 2012, 203−204, 251−256.

(51) Wang, W.-Q.; Wang, J.; Chen, J.-G.; Fan, X.-S.; Liu, Z.-T.; Liu, Z.-W.; Jiang, J.; Hao, Z. Synthesis of Novel Hyper-Cross-Linked Polymers as Adsorbent for Removing Organic Pollutants from Humid Streams. Chem. Eng. J. 2015, 281, 34−41.

(52) Liu, H.; Yu, Y.; Shao, Q.; Long, C. Porous Polymeric Resin for Adsorbing Low Concentration of VOCs: Unveiling Adsorption Mechanism and Effect of VOCs' Molecular Properties. Sep. Purif. Technol. 2019, 228, No. 115755.

(53) Shalbafan, A.; Hassannejad, H.; Rahmaninia, M. Formaldehyde Adsorption Capacity of Chitosan Derivatives as Bio-Adsorbents for Wood-Based Panels. Int. J. Adhes. Adhes. 2020, 102, No. 102669.

(54) Yang, Z.; Miao, H.; Rui, Z.; Ji, H. Enhanced Formaldehyde Removal from Air Using Fully Biodegradable Chitosan Grafted βCyclodextrin Adsorbent with Weak Chemical Interaction. Polymers 2019, 11, No. 276.

(55) Wada, T.; Uragami, T.; Matoba, Y. Chitosan-Hybridized Acrylic Resins Prepared in Emulsion Polymerizations and Their Application as Interior Finishing Coatings. J. Coat. Technol. Res. 2005, 2, 577−592.

(56) Nuasaen, S.; Opaprakasit, P.; Tangboriboonrat, P. Hollow. Latex Particles Functionalized with Chitosan for the Removal of Formaldehyde from Indoor Air. Carbohydr. Polym. 2014, 101, 179−187.

(57) Xu, D.; Zhu, R.; Xie, D.; Xie, Y.; Wu, H.; Mei, Y. AmineContaining Resin for Coating with Excellent Formaldehyde Removal Performance. Ind. Eng. Chem. Res. 2021, 60, 10674−10682.

(58) Resetco, C.; Frank, D.; Dikic, T.; Claessens, S.; Verbrugge, T.; Du Prez, F. E. Thiolactone-Based Polymers for Formaldehyde Scavenging Coatings. Eur. Polym. J. 2016, 82, 166−174.

(59) Bourguignon, M.; Thomassin, J.-M.; Grignard, B.; Jerome, C.; Detrembleur, C. Fast and Facile One-Pot One-Step Preparation of Nonisocyanate Polyurethane Hydrogels in Water at Room Temperature. ACS Sustainable Chem. Eng. 2019, 7, 12601−12610.

(60) Bourguignon, M.; Thomassin, J.-M.; Grignard, B.; Vertruyen, B.; Detrembleur, C. Water-Borne Isocyanate-Free Polyurethane Hydrogels with Adaptable Functionality and Behavior. Macromol. Rapid Commun 42 2000482. DOI: 10.1002/marc.202000482.

(61) Trézl, L.; Hullán, L.; J'szay, Z. M.; Szarvas, T.; Petneházy, I.; Szende, B.; Bocsi, J. z.; Takáts, Z.; Vékey, K.; Töke, L. Antagonistic Reactions of Arginine and Lysine against Formaldehyde and Their Relation to Cell Proliferation, Apoptosis, Folate Cycle and Photosynthesis. Mol. Cell. Biochem. 2003, 244, 167–176.

(62) Chen, N. H.; Djoko, K. Y.; Veyrier, F. J.; McEwan, A. G. Formaldehyde Stress Responses in Bacterial Pathogens. Front. Microbiol. 2016, 7, No. 257.

(63) Pinschmidt, R. K., Jr Polyvinylamine at Last. J. Polym. Sci., Part A: Polym. Chem. 2010, 48, 2257–2283.

(64) Pelton, R. Polyvinylamine: A Tool for Engineering Interfaces. Langmuir 2014, 30, 15373–15382.

(65) Zimmerer, C.; Nagel, J.; Steiner, G.; Heinrich, G. Nondestructive Molecular Characterization of Polycarbonate–Polyvinylamine Composites after Thermally Induced Aminolysis. Macromol. Mater. Eng. 2016, 301, 648–652.

(66) Panchireddy, S.; Grignard, B.; Thomassin, J. M.; Jerome, C.; Detrembleur, C. Bio-Based Poly(Hydroxyurethane) Glues for Metal Substrates. Polym. Chem. 2018, 9, 2650–2659.

(67) Panchireddy, S.; Thomassin, J. M.; Grignard, B.; Damblon, C.; Tatton, A.; Jerome, C.; Detrembleur, C. Reinforced Poly(Hydroxyurethane) Thermosets as High Performance Adhesives for Aluminum Substrates. Polym. Chem. 2017, 8, 5897–5909.

(68) Magliozzi, F.; Scali, A.; Chollet, G.; Montarnal, D.; Grau, E.; Cramail, H. Hydrolyzable Biobased Polyhydroxyurethane Networks with Shape Memory Behavior at Body Temperature. ACS Sustainable Chem. Eng. 2020, 8, 9125–9135.

(69) Gomez-Lopez, A.; Panchireddy, S.; Grignard, B.; Calvo, I.; Jerome, C.; Detrembleur, C.; Sardon, H. Poly(Hydroxyurethane) Adhesives and Coatings: State-of-the-Art and Future Directions. ACS Sustainable Chem. Eng. 2021, 9, 9541–9562.